Localized CD47 blockade enhances immunotherapy for murine melanoma

Jessica R. Ingram[a,b], Olga S. Blomberg[a], Jonathan T. Sockolosky[c,d], Lestat Ali[b], Florian I. Schmidt[a], Novalia Pishesha[a], Camilo Espinosa[a], Stephanie K. Dougan[b], K. Christopher Garcia[c,d,e], Hidde L. Ploegh[a,1,2], and Michael Dougan[a,f,2]

[a]Whitehead Institute for Biomedical Research, Massachusetts Institute of Technology, Cambridge, MA 02142; [b]Department of Cancer Immunology and Virology, Dana-Farber Cancer Institute, Boston, MA 02115; [c]Department of Molecular and Cellular Physiology, Stanford University School of Medicine, Stanford, CA 94305; [d]Department of Structural Biology, Stanford University School of Medicine, Stanford, CA 94305; [e]Howard Hughes Medical Institute, Stanford University School of Medicine, Stanford, CA 94305; and [f]Division of Gastroenterology, Department of Medicine, Massachusetts General Hospital, Boston, MA 02114

Edited by Tak W. Mak, The Campbell Family Institute for Breast Cancer Research at Princess Margaret Cancer Centre, University Health Network, Toronto, ON, Canada, and approved August 10, 2017 (received for review June 14, 2017)

CD47 is an antiphagocytic ligand broadly expressed on normal and malignant tissues that delivers an inhibitory signal through the receptor signal regulatory protein alpha (SIRPα). Inhibitors of the CD47–SIRPα interaction improve antitumor antibody responses by enhancing antibody-dependent cellular phagocytosis (ADCP) in xenograft models. Endogenous expression of CD47 on a variety of cell types, including erythrocytes, creates a formidable antigen sink that may limit the efficacy of CD47-targeting therapies. We generated a nanobody, A4, that blocks the CD47–SIRPα interaction. A4 synergizes with anti–PD-L1, but not anti-CTLA4, therapy in the syngeneic B16F10 melanoma model. Neither increased dosing nor half-life extension by fusion of A4 to IgG2a Fc (A4Fc) overcame the issue of an antigen sink or, in the case of A4Fc, systemic toxicity. Generation of a B16F10 cell line that secretes the A4 nanobody showed that an enhanced response to several immune therapies requires near-complete blockade of CD47 in the tumor microenvironment. Thus, strategies to localize CD47 blockade to tumors may be particularly valuable for immune therapy.

T cell | macrophage | cancer | protein engineering | immunotherapy

Blockade of the adaptive immune regulators CTLA-4, PD-1, and PD-L1 has shown impressive clinical efficacy across a wide range of human malignancies (1, 2). Despite the success of these adaptive checkpoint inhibitors in a subset of patients, the majority of patients still fail to achieve an adequate clinical response (1, 2). CD47 is an innate checkpoint receptor broadly expressed in normal tissues, including all cells of hematopoietic origin (3–5). CD47 negatively regulates phagocytosis, primarily through interactions with its receptor SIRP1α on macrophages (6). CD47 is up-regulated in a wide range of human and murine malignancies. Blockade of CD47 dramatically enhances antibody-dependent cellular phagocytosis (ADCP) in vitro and substantially improves antitumor responses in vivo, particularly in xenotransplant models (6–11). There are only a few examples of CD47 blockade in hosts with an intact immune system; how such interventions can synergize with immune checkpoint inhibition remains to be established (7–11). We have previously demonstrated that CD47 blockade with an alpaca-derived nanobody, in combination with a PD-L1–blocking antibody (αPD-L1) and the anti-melanoma antibody TA99, acted synergistically in the poorly immunogenic B16F10 melanoma model, while completely avoiding toxicity (7); however, whether CD47 blockade would improve the antitumor activity of alternative immune checkpoint regulators, such as CTLA-4 or PD-1, which may act via distinct mechanisms, remains unknown.

The therapeutic efficacy of αPD-L1 therapy does not rely solely on ADCP, whereas αCTLA-4 antibody therapy requires engagement of the FcγR in murine models (12, 13). In the B16F10 melanoma model, the efficacy of combination therapy with αCTLA-4 antibodies and an autologous GM-CSF–secreting tumor vaccine (GVAX) is strongly correlated with therapy-induced depletion of intratumoral regulatory T cells (Tregs). This effect is completely dependent on FcγR expression by the host (12, 13). The requirement for FcγR has been proposed to be the result of ADCP of CTLA-4–expressing Tregs by macrophages in the tumor microenvironment, although alternative antitumor mechanisms, such as antibody-dependent cellular cytotoxicity (ADCC), may also play a role (13). We hypothesized that expression of CD47 on αCTLA-4 antibody-bound cells may limit the efficacy of Treg-targeted ADCP, and that CD47 blockade may therefore improve the antitumor response.

Our previous work used A4, a high-affinity (~10 pM) blocking nanobody raised against murine CD47. A4 potently antagonizes the CD47–SIRPa interaction, while avoiding anemia, the principal toxicity of antibody-based CD47-targeting therapeutics (7). Due to their low molecular weight (~15 kDa), nanobodies have a short circulatory half-life. This expedites renal clearance and might compromise their efficacy in blocking CD47 in vivo (7, 14–16). To circumvent this pharmacokinetic limitation, we took two different approaches, generating an A4-IgG2aFc fusion protein and a B16 cell line that constitutively secretes A4. The A4-Fc fusion showed dose-limiting toxicity, whereas secretion of A4 by B16 within the tumor microenvironment achieved near-complete CD47 blockade and improved responses to the anti-melanoma antibody TA99. CD47 blockade within the tumor microenvironment also enhanced the efficacy of an

Significance

CD47 is a broadly expressed membrane-associated innate immune regulator that acts as a ligand of signal regulatory protein alpha (SIRPα) on antigen-presenting cells to inhibit phagocytosis. In xenograft models, inhibitors of the CD47–SIRPα interaction selectively target tumor-expressed CD47 and improve antibody responses to tumors by enhancing antibody-dependent cellular phagocytosis. In syngeneic settings, however, broad expression of CD47 on cells of the hematopoietic lineage creates a formidable antigen sink and increases toxicity. We find that optimal synergy between anti-CD47 antibodies and several immune therapies, including anti–CTLA-4, requires near-complete blockade of CD47 in the tumor microenvironment. Thus, novel strategies to deliver localized CD47 blockade to tumors may be particularly valuable for immune therapy.

Author contributions: J.R.I., O.S.B., J.T.S., F.I.S., S.K.D., K.C.G., H.L.P., and M.D. designed research; J.R.I., O.S.B., J.T.S., L.A., N.P., C.E., and M.D. performed research; F.I.S. contributed new reagents/analytic tools; J.R.I., O.S.B., J.T.S., L.A., F.I.S., S.K.D., K.C.G., H.L.P., and M.D. analyzed data; and J.R.I., H.L.P., and M.D. wrote the paper.

Conflict of interest statement: K.C.G. is a cofounder of Alexo, a biotechnology company focused on the clinical translation of anti-human CD47 antagonists.

This article is a PNAS Direct Submission.

[1]Present address: Program in Cellular and Molecular Medicine, Children's Hospital Boston, Boston, MA 02115.

[2]To whom correspondence may be addressed. Email: hidde.ploegh@childrens.harvard.edu or mldougan@partners.org.

This article contains supporting information online at www.pnas.org/lookup/suppl/doi:10.1073/pnas.1710776114/-/DCSupplemental.

anti-melanoma vaccine in combination with αCTLA-4 treatment. Localized CD47 blockade within the tumor microenvironment is therefore sufficient to mediate a therapeutic effect. Furthermore, our results highlight the dichotomy between αPD-L1 and αCTLA-4 responses when combined with CD47 blockade, and establish a valuable preclinical model of αCD47 toxicity in vivo.

Results

CD47 Blockade Enhances Phagocytosis of Tregs in Vitro but Not in Vivo. CD47 engagement of SIRP1α on macrophages may limit Fc-dependent depletion of Tregs by αCTLA-4 antibodies. To test this, we first cultured in vitro differentiated murine Tregs with bone marrow-derived mouse macrophages (BMDMs) in the presence or absence of αCTLA-4–blocking antibodies and A4. We quantified macrophage-mediated ADCP by flow cytometry (7). The αCTLA-4 antibody clone 9H10 promoted macrophage phagocytosis of Tregs only when coincubated with A4 (Fig. 1*A* and Fig. S1). αCTLA-4 antibody-dependent phagocytosis was not affected by antigen recognition, as phagocytosis of Tregs derived from OTII cells was equivalent when cocultured either with peptide-pulsed or with control macrophages (Fig. 1*A*). Despite the A4-dependent enhancement of Treg phagocytosis in vitro, cotreatment of mice with αCTLA-4 and A4 had no appreciable effect in vivo on Treg numbers recovered from the tumor-draining lymph nodes (Fig. 1*B*). When combined with the anti-melanoma antibody TA99 and αCTLA-4 (Fig. 1*C*) CD47 blockade with A4 did not further improve survival or reduce tumor size in the B16 melanoma model. CD47 blockade by A4, when combined with an αPD-L1–blocking antibody and TA99, slowed tumor growth and conferred a survival advantage (7) (Fig. S2). The success of combination immunotherapy involving CD47 blockade may thus depend not only on the specific checkpoint pathway targeted, but also on whether the tumor itself expresses the targeted receptor (e.g., PD-L1). Indeed, CD47 blockade with A4 did not synergize with αCTLA-4 in the context of a GVAX, a setting in which CTLA-4 is expressed only on host cells (17, 18) (Fig. 1*D* and Fig. S1).

Multiple Injections of an Anti-CD47 Nanobody Fail to Achieve Complete Blockade of CD47 in the Tumor Microenvironment. In vivo targeting of CD47 poses a challenge due to its high level of expression on cells of hematopoietic origin, including red blood cells (RBCs) and platelets. This creates a substantial antigen sink that sequesters A4 from the tumor microenvironment (3, 4). While irrelevant in xenotransplantation models where the recipient's RBCs do not usually react with species-specific αCD47 agents, this sink is a crucial pharmacodynamic variable in a syngeneic setting (4, 7–11, 19). Daily doses of 200 μg of A4 stained 50–60% of accessible CD47 on circulating hematopoietic cells (3, 4, 7, 10). Using dose escalation (Fig. 2*A* and Fig. S3) and even more frequent nanobody administration (Fig. 2*B*), we failed to achieve CD47 blockade beyond 80% on RBCs (Fig. 2 *A* and *B*). Multiple daily doses of A4 also increased CD47 blockade within the tumor microenvironment, reaching ∼75% saturation (Fig. 2*C*).

A4-IgG2a Fusion Protein Induces Severe Anemia in Mice. Because more frequent administration of A4 improved CD47 blockade, we reasoned that extension of A4 half-life by fusion to the Fc domain of murine IgG2a (A4Fc) might enhance responses, both by extending serum half-life and by increasing ADCP through FcγR engagement (Fig. 2*D* and Fig. S4*A*). Presumably, the high affinity of the monovalent A4 nanobody would be outmatched by that of the bivalent A4Fc, for avidity reasons. We nonetheless anticipated that these improvements might come at the risk of accelerated clearance of A4Fc-bound RBCs. A single dose of A4Fc induced anemia within 4 d of administration, an outcome not seen with A4 alone or with an irrelevant nanobody fused to murine IgG2a (VHHctrFc) (Fig. 2*E*). αCD47-induced anemia was not unexpected, given the rapid clearance of CD47-deficient RBCs transfused into wild-type (WT) mice, but it is not observed in xenotransplant models (3–5, 7, 8). Although Fc-dependent phagocytosis of RBCs is likely the major cause of anemia, its severity may be further enhanced by a substantial reduction in reticulocytes in A4Fc-treated mice (Fig. 2*F*). Coadministration of A4 monomer, starting on day 2, attenuated A4Fc-induced anemia and gave rise to a nearly 50% increase in hemoglobin (Fig. 2*E*), coupled with a substantial increase in the number of reticulocytes (Fig. 2*F*). We observed no differences in the numbers of white blood cells or platelets among mice treated with A4 monomer, A4Fc, or the control nanobody Fc-fusion (Fig. S4*B*). Pretreatment of animals with low doses of A4Fc (1/10th standard antibody dose: A4Fc prime) tended to alleviate

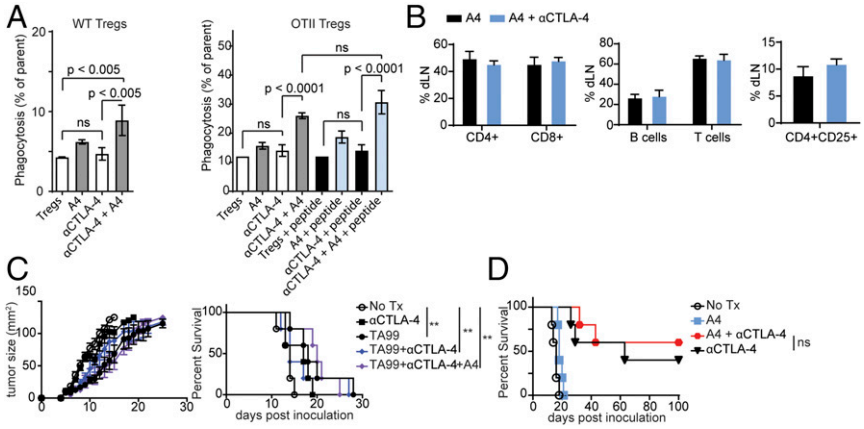

Fig. 1. CD47 blockade with the nanobody A4 enhances in vitro phagocytosis of Tregs by αCTLA-4. (*A*) BMDMs were cocultured with fluorophore-labeled in vitro differentiated Tregs for 2 h, and phagocytosis was quantified as the percentage of fluorophore-positive macrophages. (*Left*) BMDMs were cocultured with WT Tregs in the presence of αCTLA-4 Ab or αCD47 VHH (A4) as indicated. (*Right*) BMDMs were cocultured with OTII-derived Tregs in the presence of αCTLA-4 Ab, A4, or OTII peptide as indicated. Error bars indicate SEM. (*B*) Relative immune cell counts determined by flow cytometry from the tumor-draining lymph nodes of mice inoculated with B16F10 and treated with A4 or αCTLA-4 and A4 as indicated. (*C*) C57BL/6 mice were inoculated with 5×10^5 B16F10 cells by s.c. injection on day 0. On day 4, mice began antibody/nanobody treatment as indicated. (*Left*) Tumor growth curves measured by precision calipers. (*Right*) Survival curves. Error bars indicate SEM. (*D*) Survival curve for mice inoculated with B16F10 as in *C* and vaccinated with 5×10^5 irradiated GVAX cells by s.c. injection on day 0. On day 1, treatment was initiated with antibody/nanobody as indicated. In *A*–*D*, results represent at least two independent experiments.

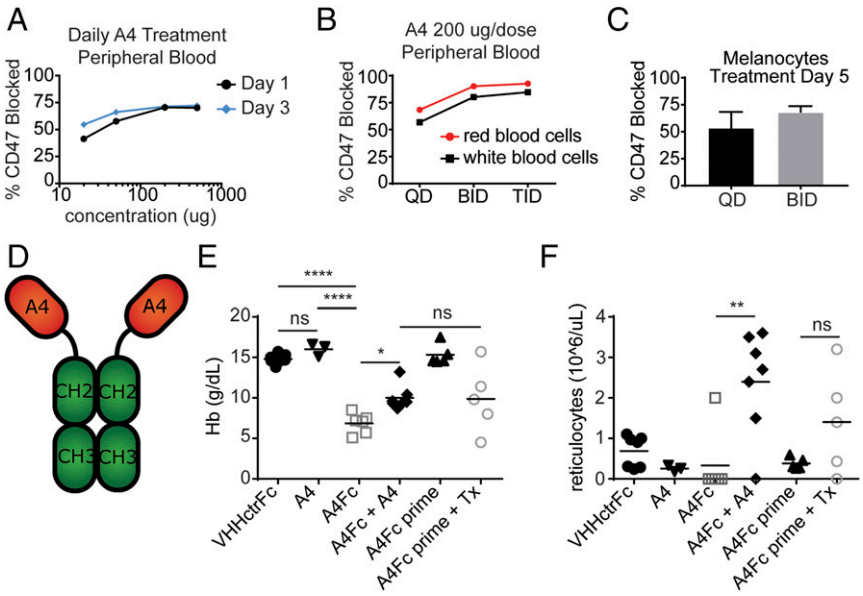

Fig. 2. A4Fc fusion induces anemia in treated mice. (*A*) Mice were treated with fluorophore-labeled A4 at the indicated concentrations for 1 or 3 d. At 24 h after the final dose, peripheral blood was collected, and the percent of CD47 blocked was determined by flow cytometry. RBC fluorescence from treated animals was compared with maximal fluorescence of RBCs from untreated animals stained ex vivo. (*B*) Mice were treated with 200 μg of fluorophore-labeled A4 at the indicated schedule and were analyzed as in *A*. QD, daily; BID, twice daily; TID, three times daily. (*C*) Mice bearing B16F10 tumors were treated with 200 μg of fluorophore-labeled A4 at the indicated schedule. After 5 d, tumors were harvested and the percent of CD47 blocked was determined as in *A*. Error bars indicate SEM. (*D*) Schematic representation of A4Fc fusion protein. (*E* and *F*) Mice were treated starting on day 0 with A4 (200 μg) daily and A4Fc/VHHctrFc (100 μg) as a single dose. For the A4Fc + A4 group, A4 was started on day 2. For the pretreatment groups (A4Fc prime), low-dose A4Fc (10 μg) was started on day −7. Tx, full-dose 100 μg A4Fc treatment on day 0. Blood was collected on day 4 and analyzed using an automated complete blood count. (*E*) Hemoglobin (Hb). (*F*) Reticulocyte count. In *A*–*C*, *E*, and *F*, the results represent two independent experiments.

anemia (Fig. 2*E*) and increased the number of reticulocytes (6, 20) (Fig. 2*F*). We did not see any therapeutic effect of the antibody at these doses. Responses to this regimen were more variable and did not reach statistical significance. The robust reticulocyte response induced by A4 on cotreatment with A4Fc suggests that reticulocytes are intrinsically less susceptible to depletion through antibody binding to CD47 or are more easily rescued than mature RBCs. The severity and rapidity of the anemia induced by A4Fc led to death in all treated animals, including tumor-bearing mice pretreated with low-dose A4Fc before receiving a therapeutic dose. Consequently, no therapeutic trials of A4Fc were able to reach a tumor endpoint, and efficacy was not directly assessable.

Local Secretion of A4 Induces Near-Complete Blockade of CD47 in the Tumor Microenvironment. To establish whether more complete blockade of CD47 in the tumor microenvironment could improve the antitumor response, we transduced B16 melanoma cells with lentiviruses encoding a secreted form of A4 (B16-A4) (Fig. 3*A*). A4 was readily detectable in tumor lysates and in supernatants of B16-A4 cells, confirming both expression and secretion of the nanobody (Fig. 3*B*). CD47 was not detectable on the surface of B16-A4 cells, but was readily detectable on cells transfected with a control nanobody (B16-ctr), consistent with autocrine binding of A4 to its target. This most likely prevents recognition of CD47 by the detection antibody, which is of considerably lower affinity (Fig. 3*C*). It is unclear whether A4 engages CD47 at the cell surface or earlier in the secretory pathway, for example, in the endoplasmic reticulum. A4 produced by B16-A4 cells not only blocked CD47 in nanobody-producing cells, but also blocked CD47 on B16 WT cells in coculture (Fig. 3*D*). Production of A4 did not affect the growth of B16 in vitro or in vivo (Fig. 3 *F* and *G*), but did enhance in vitro ADCP of tumor cells by BMDMs (6–11) (Fig. 3*E*). Preserved in vivo growth is not unexpected, given the low serum response to A4 in nanobody-treated animals (7) (Fig. S5). When injected into mice, B16-A4 cells did not cause systemic CD47 blockade, as cells isolated from the spleen and tumor-draining lymph node could be stained with CD47 antibody ex vivo (Fig. 3*H*). CD47 levels were not substantially lower on GM-CSF–secreting B16 GVAX cells delivered at a site distant from the primary B16-A4 tumor (Fig. 3*H*). Within the local tumor microenvironment, B16-A4 tumors showed near-complete blockade of CD47 both on tumor-infiltrating leukocytes (TILs) and B16 itself (Fig. 3*I*). Presumably, given the short plasma half-life of nanobodies, any surplus A4 that reaches the circulation is rapidly cleared.

Secretion of A4 Within the Tumor Microenvironment Enhances Responses to Anti-Tumor Antibodies. We next examined the consequences of near-complete CD47 blockade within the tumor microenvironment. Treatment of B16-A4 cells with TA99 modestly delayed tumor growth when administered after tumors were first palpable (Fig. 4*A* and Fig. S6*A*), and cleared tumors when given on the day after inoculation (Fig. 4*B* and Fig. S6*B*). Thus, local blockade of CD47 is sufficient for a therapeutic effect. Systemic administration of αCD47 mostly targets the antigen sink, fails to enhance ADCP, and underscores the importance of reaching near-complete CD47 blockade in the tumor to achieve optimal protection.

We next investigated the importance of adaptive immunity in a response to day 1 TA99 treatment. Neither deficiency in the transcription factor BATF3 (Fig. 4*C* and Fig. S6*C*), required for efficient cross-presentation by DCs, nor deletion of RAG2 (Fig. 4*D* and Fig. S6*D*) to completely ablate adaptive immunity affected the response of B16-A4 to TA99. Therefore, adaptive responses are dispensable for clearing early-stage B16F10 tumors. This is in contrast to eradication of established tumors, where effective antitumor responses depend on the modulation of adaptive responses (7, 11, 21).

Local CD47 Blockade Improves Responses to CTLA-4 GVAX. We next investigated whether local CD47 blockade enhanced responses to the GVAX tumor vaccine. GVAX treatment modestly increased

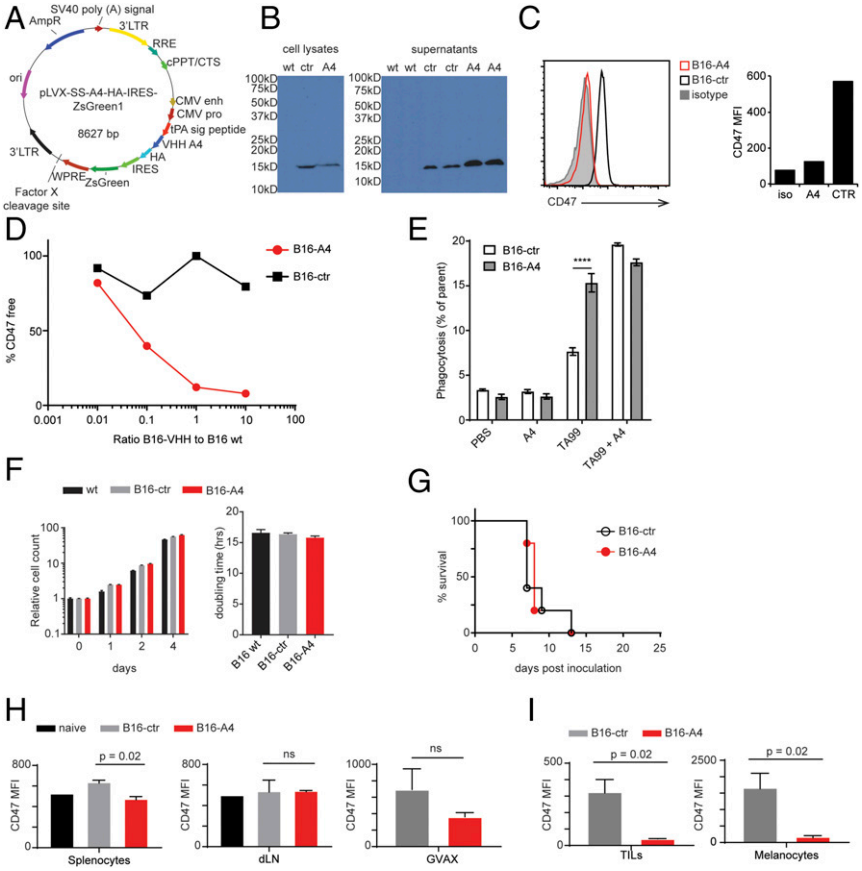

Fig. 3. Autocrine secretion of A4 effectively blocks CD47 in the tumor microenvironment. (*A*) Vector map of the lentiviral vector used to produce VHH-secreting B16F10 cell lines. (*B*) Anti-HA immunoblots for HA-tagged VHHs in the lysates (*Left*) and supernatants (*Right*) from B16F10 cells engineered to produce A4 (B16-A4) or a control nanobody (B16-ctr). (*C*) CD47 flow cytometry on B16-A4 and B16-ctr cells. (*Left*) Histogram. (*Right*) Quantification of CD47 maximum fluorescent intensity (MFI). (*D*) B16-A4 or B16-ctr cells were cocultured with WT cells at the indicated ratios. After 24 h of culture, surface-detectable CD47 was analyzed on the WT cells. The percent of bound CD47 was determined by comparing CD47 fluorescence on cocultured WT cells with the maximum CD47 fluorescence on WT cells grown alone. (*E*) B16 cells were cocultured with BMDMs as in Fig. 1*A* in the presence of absence of the indicated antibody or VHH. Phagocytosis was analyzed as in Fig. 1*A*. (*F*) Relative cell counts over time in days (*Left*) and doubling time (*Right*) for B16-ctr, B16-A4, and WT cells as measured by CellTiterGlo. (*G*) Survival curve for mice inoculated with 5×10^5 B16F10-derived cell lines as indicated on day 0. (*H* and *I*) Mice were inoculated with B16F10-derived cell lines as in *G*. On day 10, the indicated organs (*H*) or tumors (*I*) were harvested and analyzed for accessibility of CD47 to staining by flow cytometry. Graphs depict CD47 MFI normalized to the MFI of an isotype control (subtracted). In *D–F*, *H*, and *I*, error bars indicate SEM. In *B–I*, results represent at least two independent experiments.

survival in mice inoculated with B16-A4, but not in those inoculated with B16-ctr (Fig. 4*E* and Fig. S6*E*). To determine whether local blockade of CD47 could be effective against large, established tumors, mice with B16-A4 or B16-ctr tumors were vaccinated with GVAX, and the tumors were allowed to grow to palpable size (day 8) before treatment with αCTLA-4. Even in this setting, local secretion of A4 provided a substantial therapeutic benefit (7, 17) (Fig. 4*F* and Fig. S6*F*). Although local delivery of A4 was effective, GVAX-αCTLA-4 in combination with A4Fc caused considerable toxicity (Fig. 4*G*). Thus, alternative strategies for enhancing blockade of CD47 in the tumor microenvironment, without having to resort to the addition of an Fc portion, may be useful in combination with certain immune therapies, such as GVAX (12, 13, 22, 23).

Discussion

Blockade of the innate immune checkpoint regulator CD47 has demonstrated impressive preclinical efficacy in a wide variety of xenotransplant models, and more recently against syngeneic tumors (7–13). The use of syngeneic tumor models has two critical advantages for studying the impact of immune interventions that target CD47: it enables evaluation of combination therapies that target the adaptive immune system, and it provides insight into potential toxicities that arise from expression of CD47 on non-malignant tissues (7, 11, 13). The wide expression of CD47 serves as a formidable antigen sink that limits the efficacy of CD47-targeted therapies. Optimal antitumor responses to GVAX, antitumor antibody, and αCTLA-4 therapy in the B16 mouse melanoma model all require near-complete CD47 blockade within the tumor microenvironment but not at distal sites, including the tumor-draining lymph nodes. However, dependence on near-complete CD47 blockade for effective combination immunotherapy is not universal. Combination treatment by systemic αCD47 nanobody administration with αPD-L1 is effective (7). Although the mechanism underlying the differential requirement for CD47 blockade in αCTLA-4 and αPD-L1 therapy is not clear, it likely depends on the cell type targeted. CTLA-4 is expressed on activated and regulatory T cells, while PD-L1 can be expressed on multiple cell types, including tumor cells themselves (1, 7, 12, 13, 24).

To date, therapeutic responses to CD47 blockade have targeted malignant tissues and have not been used successfully to enhance ADCP of host cells to favor tumor growth, such as Tregs. While both tumor cells and normal immune cells are

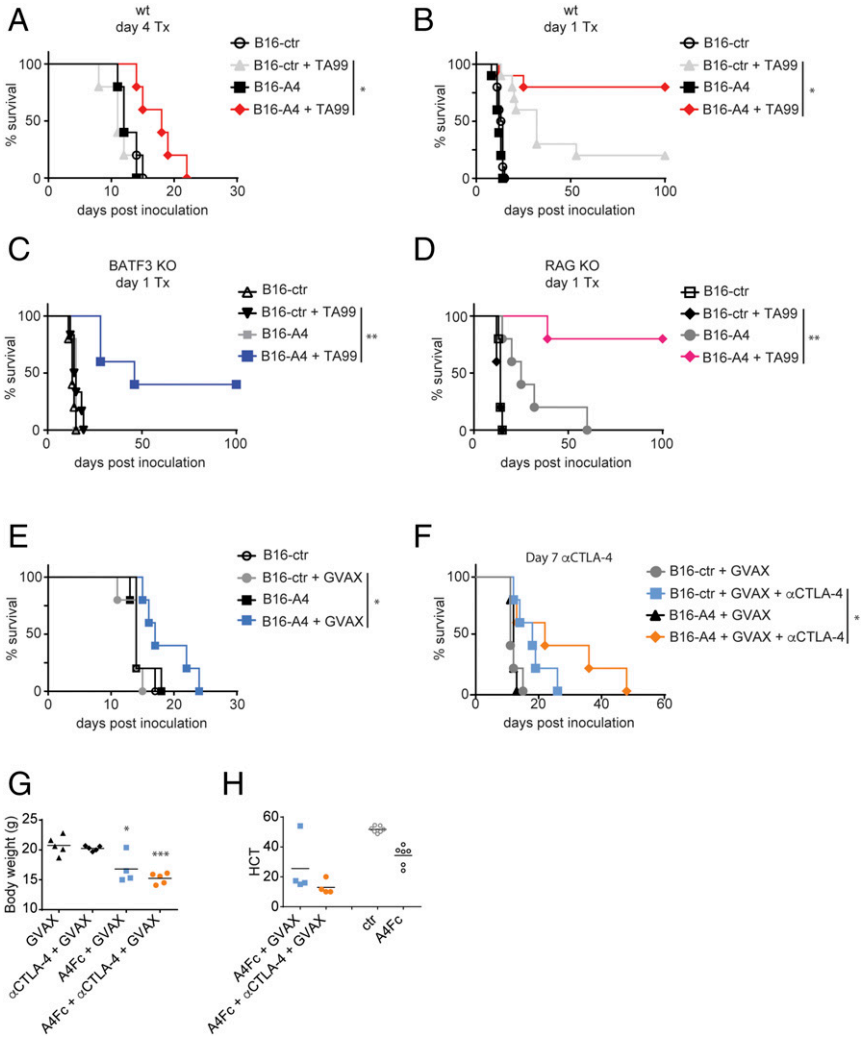

Fig. 4. Local secretion of a CD47-blocking nanobody enhances antimelanoma immune therapy. (*A–F*) Survival curves for mice inoculated with 5×10^6 B16F10-derived cells by s.c. injection on day 0 and treated as indicated. (*A*) WT (wt) mice were treated on day 4 with TA99 or were left untreated. Results are representative of two independent experiments. (*B–D*) WT (*B*), BATF3 KO (*C*), and RAG KO (*D*) mice were treated in parallel on day 1 with TA99 or were left untreated. Results represent the combined results from two cohorts treated in parallel. (*E*) WT mice received GVAX on day 0 or were left untreated. (*F*) WT mice received GVAX on day 0; on day 7, mice began treatment with αCTLA-4 antibody or were left untreated. (*G*) Body weights of mice inoculated with 5×10^6 B16F10-derived cells and vaccinated with GVAX on day 0, and then treated with αCTLA-4 antibody, A4Fc, or αCTLA-4 + A4Fc or left untreated 3 d before measurement. $*P < 0.05$, $***P < 0.0001$ compared with GVAX alone. In *E* and *F*, results are representative of at least two independent experiments. (*H*) Hematocrit (HCT) from mice treated with A4Fc or αCTLA-4 + A4Fc and analyzed at 3 d after dosing as in *G*. For comparison, HCT measurements from control-treated (ctr) and A4Fc-treated animals from a separate cohort are presented alongside.

susceptible to ADCP in vitro, we found no evidence that Tregs were targeted in vivo during CD47 blockade. This may be a limitation of targeting Tregs through αCTLA-4, or may represent a more fundamental resistance to ADCP of this cell type, potentially through the engagement of additional antiphagocytic pathways. The normal circulatory half-life of CD47-deficient erythrocytes in CD47-deficient mice shows that such pathways exist. CTLA-4 is a low- abundance protein that is maintained largely in intracellular stores, and thus may fail to reach the surface density threshold required for ADCP.

In principle, the use of autologous nanobody secretion could introduce a tumor antigen that might complicate immune therapy, but we find little evidence for this in our model. B16 cells engineered to secrete A4 grow normally in mice. Although this may change in the setting of immune therapy, we used cells engineered to secrete a nanobody of irrelevant specificity as a control. Since most anti-nanobody responses are to the conserved framework regions, this control directly addresses this concern. In addition, through an analysis of serum anti-nanobody responses, we have found that A4 is particularly nonimmunogenic, possibly due to its tendency to bind RBCs, a tolerance-inducing regimen (7, 25). Therefore, if anti-nanobody responses were the principal cause of the effect of local delivery, then we would expect the control cells secreting the irrelevant nanobody to be more rapidly rejected.

Our findings concerning the toxicity of CD47 blockade are relevant to understanding potential side effects of CD47 antagonists in patients. By creating A4Fc, a fusion between the A4 nanobody and the murine IgG2a Fc region, we produced a reagent that binds and blocks CD47 with low picomolar affinity, while retaining the ability to engage FcγR. Thus, A4Fc can activate macrophage phagocytosis, as well as potentially initiate ADCC. In vivo administration of A4Fc led to rapid and significant anemia that worsened when combined with other forms of immune therapy. Given that RBCs express CD47 on their surface, where it plays an important role in their clearance, this finding was perhaps expected (4).

αCD47-induced anemia is not observed in xenotransplantation models, where host CD47 is immunologically distinct from CD47 on the tumor. Therefore, the therapeutic reagents used to target CD47 on the tumor are tumor-specific and do not target host cells. In the previously reported syngeneic models, the antibodies used either lacked an Fc or were of considerably lower affinity than the A4 nanobody and its derivatives used in our study. Thus, we have established a murine model of αCD47-induced anemia. This model should provide a platform not only for studying potential therapeutic strategies for mitigating anemia, as explored here, but also to evaluate αCD47 toxicity in the course of combination immunotherapy. Combination immunotherapy is likely to be critical to achieving a meaningful therapeutic effect of CD47 blockade against many tumors, as we and others have found.

Published data from human clinical trials of CD47 blockade are not yet available, but findings in nonhuman primates demonstrated a treatment-related anemia that was manageable at the doses of αCD47 antibody used (20). In those studies, the antibody was shown to bind human and nonhuman primate CD47 with equal affinity. The study also showed that the antibody could reach serum drug levels that were previously effective in xenotransplant models without inducing substantial toxicity (20). However, this finding is limited by the use of a xenotransplant model to determine an effective drug dose. Since mice obviously lack endogenous expression of xenogeneic CD47, they also lack a circulating antigen sink in xenotransplant models. The presence of this antigen sink almost certainly alters the relationship between the drug level in the serum, and the level within the tissues and tumor. Without either knowing the effective tissue concentration of antibody, or demonstrating both safety and efficacy in nonhuman primates or patients, the extent to which toxicity will limit the effectiveness of antibody-based CD47 targeting therapies is presently unclear. We developed a nanobody against CD47 as an alternate strategy for blocking this pathway that does not risk systemic toxicities, even when given at therapeutic doses, but our findings serve as a cautionary note. Nanobodies, or other high-affinity receptor-binding therapies that lack an Fc domain, are an effective means for avoiding toxicity, but are limited by circulatory half-life. Based on measurements of several other nanobodies, A4 is likely to have a serum half-life of <30 min, although its tissue half-life is considerably longer, as we demonstrate here (14). For this reason, it cannot achieve the steady state serum drug levels reported in the xenotransplant and nonhuman primate models using standard injections. We suggest that alternative delivery mechanisms for nanobodies may be necessary to achieve adequate blockade of highly expressed targets, particularly in settings where inclusion of an Fc increases toxicity. Potential strategies to translate nanobody-based CD47 blockade into a clinical setting could include increasing serum half-life through PEGylation or fusion to albumin, direct injection into the tumor, or incorporation into drug-releasing depots that could produce a continuous supply of nanobody in the circulation (7, 22, 23).

Methods

All animals were maintained according to protocols approved by either MIT's Committee on Animal Care or the Dana-Farber Cancer Institute's Institutional Animal Care and Use Committee. Methods for expression and VHH and fusion proteins followed standard procedures as described previously (7). Immunological assays and in vivo tumor experiments followed procedures described elsewhere (7). For Details of all experiments are provided in *SI Methods*.

ACKNOWLEDGMENTS. We thank Monique J. Kauke and K. Dane Wittrup for the TA99 antibody, Mohammad Rashidian for helpful discussions, Elisa Bello for technical assistance, and the staff of the flow cytometry facility at Whitehead Institute. Funding was provided by the Ludwig Cancer Research Postdoctoral Fellowship and the Claudia Adams Barr Program for Innovative Cancer Research (to J.R.I.); Maag, Lever, Darm Stichting, and the Bekker-La Bastide Fonds (to O.S.B.); National Institutes of Health (NIH) Training Grant 5T32 AI072905 and a PhRMA Translational Medicine and Therapeutics Postdoctoral Fellowship (to J.T.S.); the Melanoma Research Alliance (to S.K.D.); NIH Grant R01 CA177684, the Howard Hughes Medical Institute, and the Ludwig Foundation (to K.C.G.); NIH Grants R01 AI087879-06, DP1 GM106409-03, and R01 GM100518-04 and the Lustgarten Foundation (to H.L.P.); and NIH Training Grant 1F32CA210568-01 and NIH Center for the Study of Inflammatory Bowel Disease Pilot Grant DK043351 (to M.D.).

1. Baumeister SH, Freeman GJ, Dranoff G, Sharpe AH (2016) Coinhibitory pathways in immunotherapy for cancer. *Annu Rev Immunol* 34:539–573.
2. Gotwals P, et al. (2017) *Dranoff Chemo+IT Review* (Nature Publishing Group, London), pp 1–16.
3. Weiskopf K (2017) Cancer immunotherapy targeting the CD47/SIRPα axis. *Eur J Cancer* 76:100–109.
4. Barclay AN, Van den Berg TK (2014) The interaction between signal regulatory protein alpha (SIRPα) and CD47: Structure, function, and therapeutic target. *Annu Rev Immunol* 32:25–50.
5. Ho CCM, et al. (2015) "Velcro" engineering of high affinity CD47 ectodomain as signal regulatory protein α (SIRPα) antagonists that enhance antibody-dependent cellular phagocytosis. *J Biol Chem* 290:12650–12663.
6. Willingham SB, et al. (2012) The CD47-signal regulatory protein alpha (SIRPa) interaction is a therapeutic target for human solid tumors. *Proc Natl Acad Sci USA* 109: 6662–6667.
7. Sockolosky JT, et al. (2016) Durable antitumor responses to CD47 blockade require adaptive immune stimulation. *Proc Natl Acad Sci USA* 113:E2646–E2654.
8. Weiskopf K, et al. (2013) Engineered SIRPα variants as immunotherapeutic adjuvants to anticancer antibodies. *Science* 341:88–91.
9. Majeti R, et al. (2009) CD47 is an adverse prognostic factor and therapeutic antibody target on human acute myeloid leukemia stem cells. *Cell* 138:286–299.
10. Jaiswal S, et al. (2009) CD47 is upregulated on circulating hematopoietic stem cells and leukemia cells to avoid phagocytosis. *Cell* 138:271–285.
11. Liu X, et al. (2015) CD47 blockade triggers T cell-mediated destruction of immunogenic tumors. *Nat Med* 21:1209–1215.
12. Selby MJ, et al. (2013) Anti-CTLA-4 antibodies of IgG2a isotype enhance antitumor activity through reduction of intratumoral regulatory T cells. *Cancer Immunol Res* 1: 32–42.
13. Simpson TR, et al. (2013) Fc-dependent depletion of tumor-infiltrating regulatory T cells co-defines the efficacy of anti-CTLA-4 therapy against melanoma. *J Exp Med* 210:1695–1710.
14. Rashidian M, et al. (2015) Noninvasive imaging of immune responses. *Proc Natl Acad Sci USA* 112:6146–6151.
15. Muyldermans S (2013) Nanobodies: Natural single-domain antibodies. *Annu Rev Biochem* 82:775–797.
16. Van Audenhove I, Gettemans J (2016) Nanobodies as versatile tools to understand, diagnose, visualize and treat cancer. *EBioMedicine* 8:40–48.
17. van Elsas A, Hurwitz AA, Allison JP (1999) Combination immunotherapy of B16 melanoma using anti-cytotoxic T lymphocyte-associated antigen 4 (CTLA-4) and granulocyte/macrophage colony-stimulating factor (GM-CSF)-producing vaccines induces rejection of subcutaneous and metastatic tumors accompanied by autoimmune depigmentation. *J Exp Med* 190:355–366.
18. Dougan M, et al. (2010) IAP inhibitors enhance co-stimulation to promote tumor immunity. *J Exp Med* 207:2195–2206.
19. Theocharides APA, et al. (2012) Disruption of SIRPα signaling in macrophages eliminates human acute myeloid leukemia stem cells in xenografts. *J Exp Med* 209: 1883–1899.
20. Liu J, et al. (2015) Pre-clinical development of a humanized anti-CD47 antibody with anti-cancer therapeutic potential. *PLoS One* 10:e0137345.
21. Zhu EF, et al. (2015) Synergistic innate and adaptive immune response to combination immunotherapy with anti-tumor antigen antibodies and extended serum half-life IL-2. *Cancer Cell* 27:489–501.
22. Sockolosky JT, Szoka FC (2015) The neonatal Fc receptor, FcRn, as a target for drug delivery and therapy. *Adv Drug Deliv Rev* 91:109–124.
23. Dougan M, Dougan SK (2017) Targeting immunotherapy to the tumor microenvironment. *J Cell Biochem* 118:3049–3054.
24. Keir ME, Butte MJ, Freeman GJ, Sharpe AH (2008) PD-1 and its ligands in tolerance and immunity. *Annu Rev Immunol* 26:677–704.
25. Pishesha N, et al. (2017) Engineered erythrocytes covalently linked to antigenic peptides can protect against autoimmune disease. *Proc Natl Acad Sci USA* 114: 3157–3162.